CHAPTER V
UNCERTAINTY MODELING AND STOCHASTIC ANALYSIS FOR OMES-WSPHS INTEGRATION

5.1 General Introduction

In this chapter, the OMES-WSPHS integration is utilized as a stochastic analysis model to account for uncertainty variables, including fluctuations in weather modeled using Weibull distribution to represent RE generation and variations in end-user behavior to model multi-energy demand. The proposed approach minimizes TOC while ensuring system reliability and operational feasibility under uncertain conditions. The methodology employs a stochastic optimization process, leveraging MCS to handle uncertainties associated with renewable energy sources and energy demand variations. This chapter presents the performance evaluation of the proposed method and its effectiveness in achieving an optimal scheduling strategy for MES.

5.2 Problem Formulation

The mathematical formulation remains consistent with the previous chapter, ensuring that the optimization framework aligns with the problem structure in Chapter 3. Therefore, the objective function and constraints are retained as follows: Refer to Equations (3.21)–(3.31).

5.2.1 Uncertainty Variable Formulation

This section identifies the uncertainty variables considered in OMES-WSPHS integration, including wind speed, solar irradiance, electricity load, and heat load. It also outlines the process of extracting historical data to generate uncertainty

data sets for solar and wind. In contrast, due to the lack of historical data, the uncertainty in electricity and heat load is modeled using percentage-based standard deviation assumptions. To formulate the probabilistic wind speed and solar irradiance model, the historical annual data need to extracted hour-by-hour in for reflects the fluctuation in that hour (Chayakulkheeree, 2013). Figure 5.1 shows the probabilistic wind speed and solar irradiance model preparation.

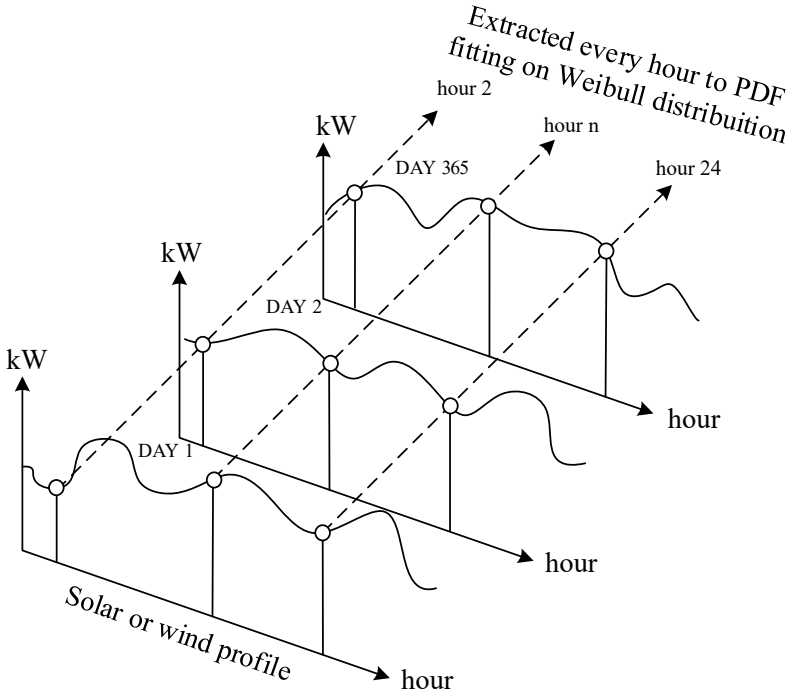

Figure 5.1 The probabilistic wind speed and solar irradiance model preparation, adapted from Chayakulkheeree (2013)

The historical annual data of wind speed and solar irradiance are analyzed to determine their mean and variability. The mean value and its range (mean – SD to mean + SD) for solar irradiance are presented in Fig. 5.2 (subplot 1), while the corresponding power output from PVPs is shown in Fig. 5.2 (subplot 2). Similarly, the mean and its range for wind speed are illustrated in Fig. 5.3 (subplot 1), with the power

output from WTs displayed in Fig. 5.3 (subplot 2). For both power output, using the power conversion equations from Chapter 3 (Eq. 3.3–3.5). Figures 5.4 and 5.5 present box plots to illustrate the statistical distribution of data for solar energy and wind energy, respectively. The construction of model the variability of wind speed and solar irradiance, the Weibull distribution is fitted to the data. The PDF of the solar irradiance and wind speed can be modeled in Weibull distribution as shown in Eq. (5.1) and Eq. (5.2), respectively. The key parameters for this distribution are the shape and scale factors, which vary hourly to account for fluctuations. The corresponding shape and scale values for each hour are listed in Table 5.1. Using these parameters, random values are generated based on the Weibull distribution.

$$f_{SI}(SI) = \frac{b_{SI}}{a_{SI}}\left(\frac{SI}{a_{SI}}\right)^{b_{SI}-1} e^{-\left(\frac{SI}{a_{SI}}\right)^{b_{SI}}}, \tag{5.1}$$

$$f_{v_{WTs}}(v_{WTs}) = \frac{b_{v_{WTs}}}{a_{v_{WTs}}}\left(\frac{v_{WTs}}{a_{v_{WTs}}}\right)^{b_{v_{WTs}}-1} e^{-\left(\frac{v_{WT}}{a_{WT}}\right)^{b_{v_{WTs}}}}. \tag{5.2}$$

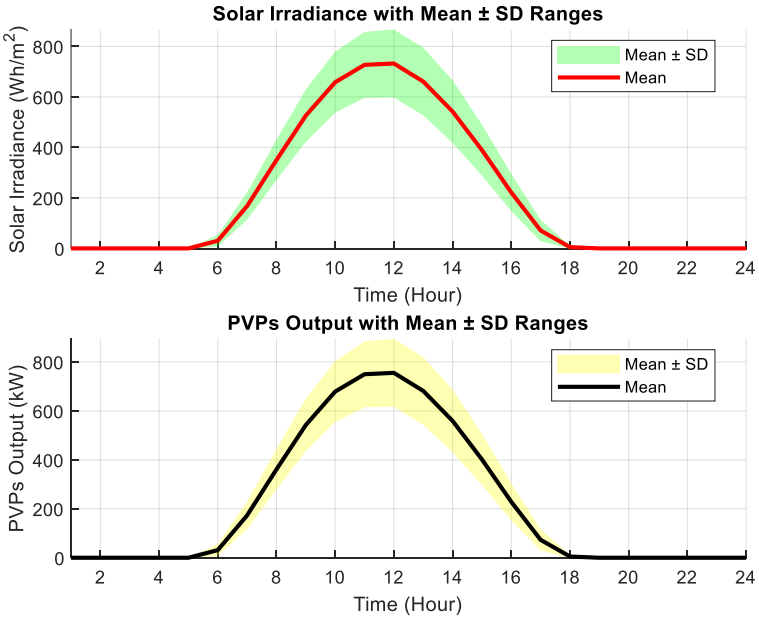

Figure 5.2 Mean, variability (Mean ± SD) of solar irradiance, and power output from PVPs

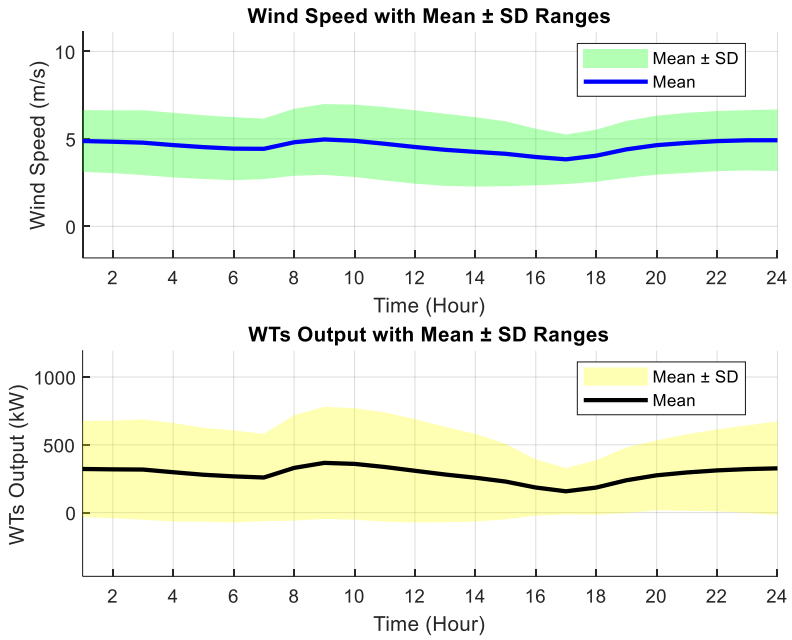

Figure 5.3 Mean, variability (Mean ± SD) of wind speed, and power output from WTs

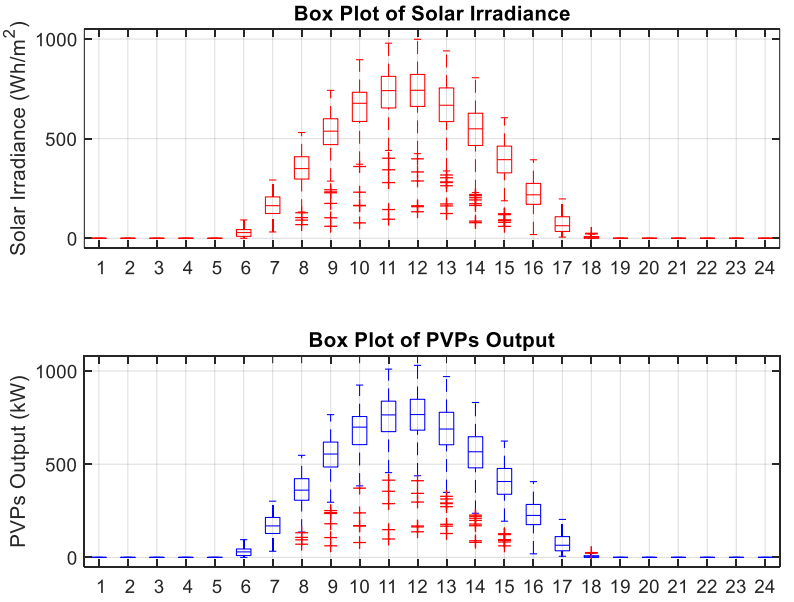

Figure 5.4 The box plots of solar irradiance and power output from PVPs

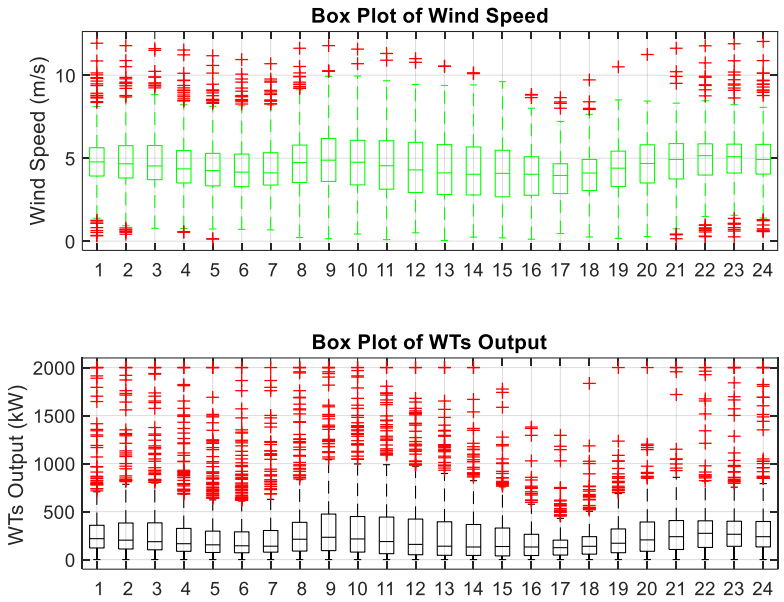

Figure 5.5 The box plots of wind speed and power output from WTs

Table 5.1 The corresponding shape and scale values of wind and solar for each hour

Hour	Solar irradiance (Wh/m^2)		Wind speed (m/s)	
	Shape (*a*)	Scale (*b*)	Shape (*a*)	Scale (*b*)
1	0	0	2.899	5.47
2	0	0	2.83	5.411
3	0	0	2.729	5.367
4	0	0	2.656	5.223
5	0	0	2.611	5.088
6	1.574	37.981	2.616	5.004
7	3.417	187.173	2.708	4.98
8	5.008	381.229	2.662	5.401
9	6.103	566.063	2.621	5.585
10	6.673	704.946	2.528	5.506
11	6.682	778.166	2.388	5.322
12	6.51	784.897	2.306	5.124

Table 5.1 The corresponding shape and scale values of wind and solar for each hour (Continued)

Hour	Solar irradiance (Wh/m^2)		Wind speed (m/s)	
	Shape (*a*)	Scale (*b*)	Shape (*a*)	Scale (*b*)
13	5.87	712.703	2.225	4.928
14	5.142	588.970	2.278	4.806
15	4.464	426.838	2.386	4.678
16	3.335	246.762	2.643	4.454
17	1.727	79.791	2.929	4.287
18	1.785	10.216	2.924	4.518
19	0	0	2.943	4.927
20	0	0	3.004	5.184
21	0	0	2.989	5.316
22	0	0	3.042	5.425
23	0	0	3.042	5.482
24	0	0	2.96	5.493

Electricity and heat loads can be modeled using a normal distribution PDF, as this approach effectively captures the typical energy consumption patterns observed in industrial applications. The PDF representing the normal distribution of electricity and heat loads are given in Eq. (5.3) and (5.4), respectively.

$$f_{L_E}(L_E) = \frac{1}{\sqrt{(2\pi)\sigma_{L_E}}} \exp\left(-\frac{(L_E - M_{L_E})^2}{2\sigma_{L_E}} \right), \tag{5.3}$$

$$f_{L_H}(L_H) = \frac{1}{\sqrt{(2\pi)\sigma_{L_H}}} \exp\left(-\frac{(L_H - M_{L_H})^2}{2\sigma_{L_H}} \right). \tag{5.4}$$

In this study, due to the absence of historical data, a percentage-based standard deviation assumption is adopted. Specifically, the mean values of electricity and heat load data are defined in Chapter 3, as shown in Fig. 3.4. The standard deviation is set at 2% of the mean value for each energy demand. The electricity and

heat loads are generated using the normal distribution model, their mean values and corresponding ranges (mean ± SD, mean ± 2SD, and ± 3SD) are illustrated in Fig. 5.6, where (a) represents electricity load and (b) represents heat load. Finally, the box plot for illustration of the statistical distribution of data for multi-energy loads can be shown in Fig. 5.7.

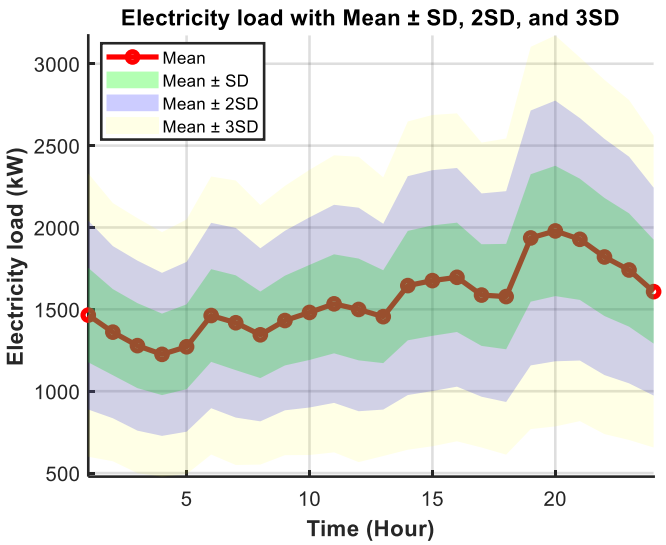

(a)

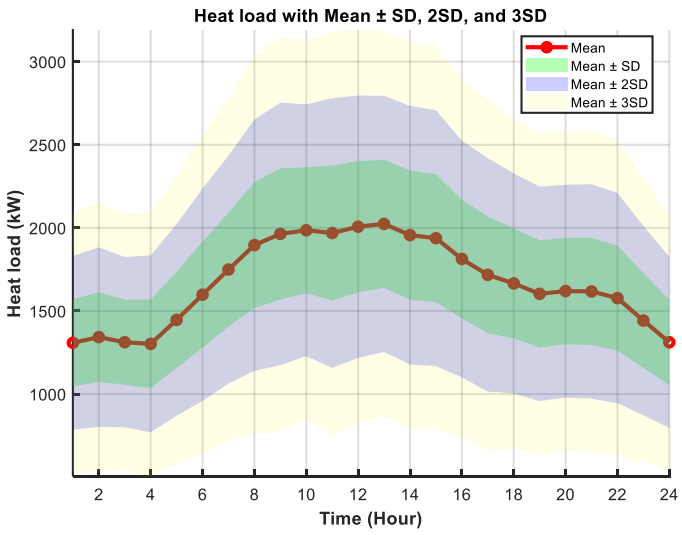

(b)

Figure 5.6 The mean values and corresponding ranges (mean ± SD, mean ± 2SD, and ± 3SD) for (a) electricity load and (b) heat load

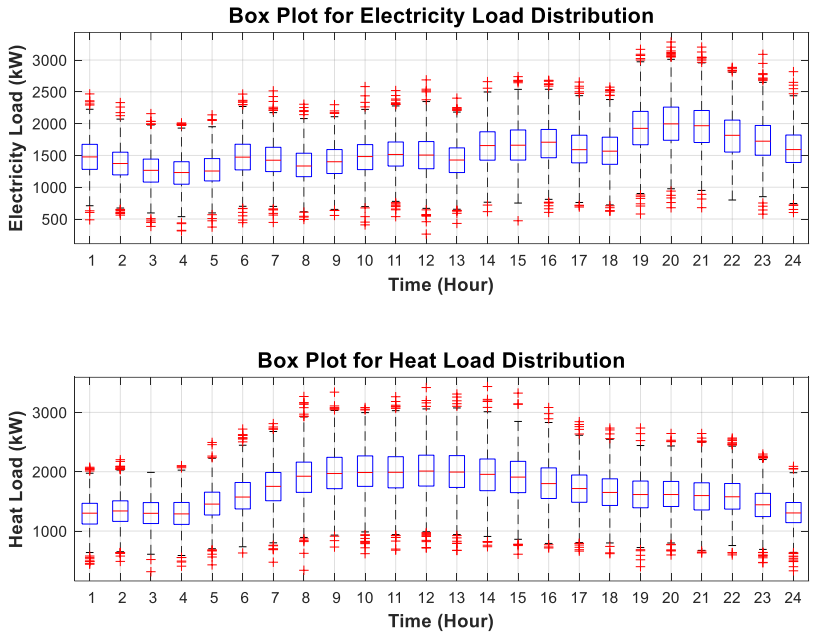

Figure 5.7 The box plots of electricity load and heat load

5.2.2 Probabilistic Technique Based on MCS

MCS has become a fundamental technique for modeling uncertainty in modern power systems. It is particularly valuable for its ability to handle high-dimensional and nonlinear problems, which are commonly encountered in integrated energy systems with renewable energy sources. These systems often exhibit inherent variability due to the intermittent nature of renewable resources such as wind and solar power. The core principle of MCS involves performing a large number of simulations based on random sampling from probability distributions that describe the behavior of uncertain input variables (Metropolis & and Ulam, 1949). In probabilistic modeling of power and multi-energy systems, uncertain variables such as RE generation, load demand, and electricity market prices are typically represented using probability distributions derived from historical data. These distributions are selected to best reflect the statistical characteristics and variability of each parameter. Common choices include normal, log-normal, Weibull, beta, and gamma distributions,

depending on the data properties. MCS utilizes these distributions to generate numerous random scenarios, enabling a comprehensive evaluation of system performance under uncertainty without relying on overly simplified assumptions. This approach provides system planners with the ability to account for a wide range of possible outcomes and make more informed and flexible decisions.

Each scenario generated by MCS represents a possible state of the system under a specific realization of uncertainty. These scenarios are processed through optimization models or system simulators to determine corresponding outputs, such as total operating cost, carbon emissions, reliability indices, or voltage stability margins. Statistical analysis of the results provides valuable insights into how uncertainties impact system performance. By integrating MCS into the modeling framework, the proposed approach enhances the robustness of scheduling decisions and allows system operators to prepare for a wide spectrum of potential operating conditions. This methodology not only supports risk-aware planning but also strengthens the flexibility and resilience of future intelligent energy systems.

5.3 Stochastic Analysis for OMES-WSPHS Using MCS

In this section, MCS is applied to evaluate the impact of uncertainty in the OMES-WSPHS. Given the stochastic nature of wind and solar power generation, electricity and heat demand, and HS scheduling, MCS is utilized to assess system performance under various realizations of these uncertainties. The process begins by defining probability distributions for key uncertain parameters, such as wind and solar power fluctuations modeled using a Weibull distribution and electricity and heat demand variations modeled using a normal distribution. Random samples are then generated based on these distributions, and each sampled scenario is used to solve the OMES-WSPHS optimization problem. In this study, the MCS is set to run for 500 iterations to ensure sufficient statistical representation of uncertainties. After completing the final iterations, it is necessary to verify the convergence of the

cumulative mean. The error of the cumulative mean can be determined based on the percentage calculation of the previous final iteration and the final iteration. If the resulting error is less than 1%, it indicates that the solution has successfully converged. A flowchart illustrating the MCS procedure for OMES-WSPHS is presented in Fig. 5.8.

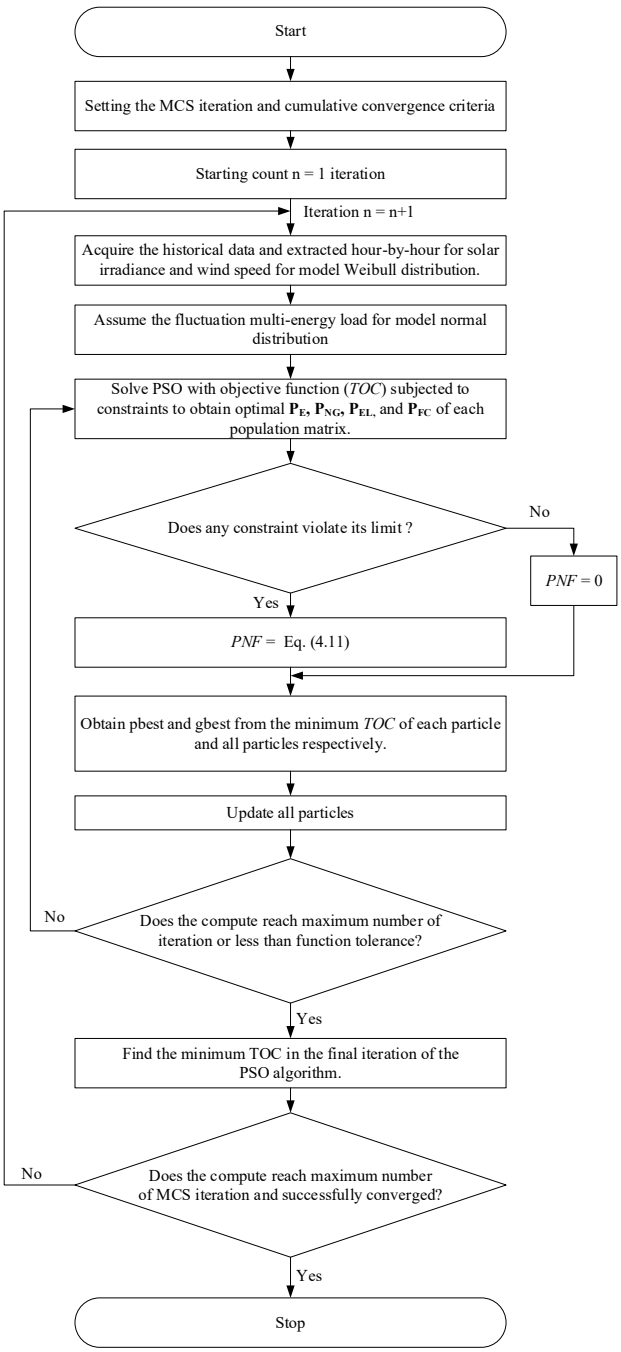

Figure 5.8 The flow chart of MCS procedure for OMES-WSPHS

The randomly sampled solar irradiance values are illustrated in Fig. 5.9, while the wind speed values are depicted in Fig. 5.10, leading to the corresponding electrical power output shown in Fig. 5.11. Additionally, both energy loads incorporate the uncertainty data from Fig. 5.6. Ultimately, all uncertainty parameters are considered as variable power generation inputs for determining the probabilistic solution. The results from multiple iterations are collected and analyzed using statistical measures, offering valuable insights into the feasibility of multi-energy scheduling under uncertainty.

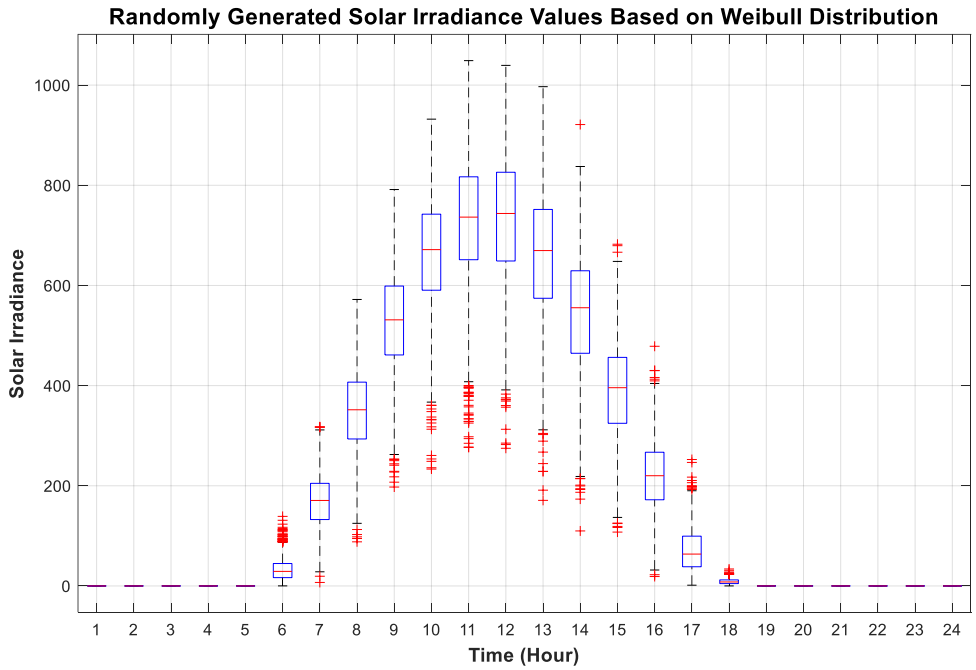

Figure 5.9 The box plot of Randomly generated solar irradiance values based on the Weibull distribution

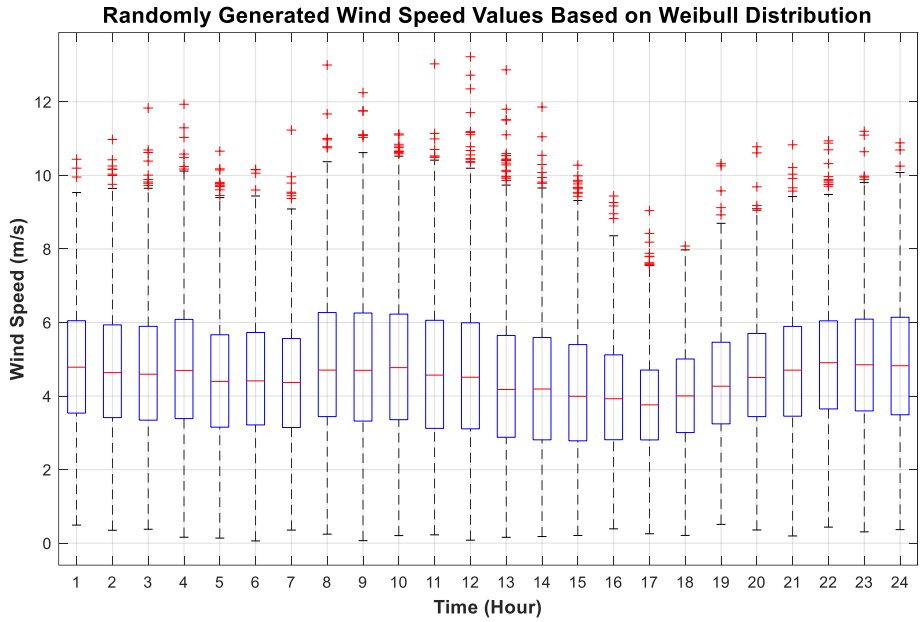

Figure 5.10 The box plot of Randomly generated wind speed values based on the Weibull distribution

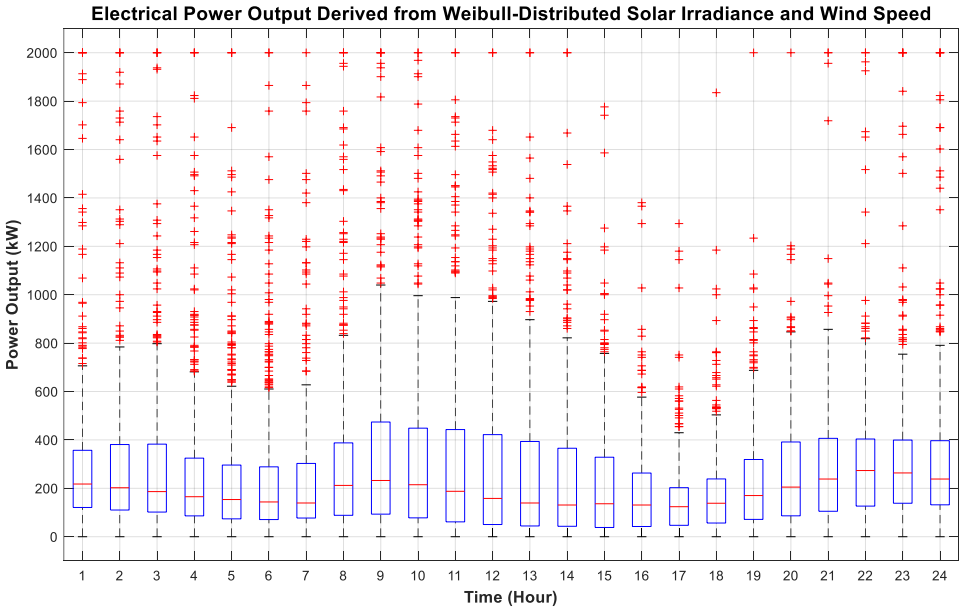

Figure 5.11 The box plot of electrical power output derived from Weibull-distributed solar irradiance and wind speed

5.4 Simulation Results

The cumulative mean of TOC over 500 iterations, as shown in Fig. 5.12, demonstrates the convergence behavior of the stochastic optimization process, specifically MCS. The results indicate a rapid initial decline in TOC, followed by stabilization after approximately 150 iterations. Beyond 300 iterations, TOC remains steady. Notably, when MCS reaches 500 iterations, the cumulative mean error defined as the difference between the previous final iteration and the final iteration falls to 0.0019%, below the 1% threshold, confirming that additional calculations are unnecessary. This demonstrates that the stochastic modeling approach handles uncertainty within the OMES-WSPHS integration. Consequently, the proposed framework minimizes operational costs while maintaining stability under uncertain conditions.

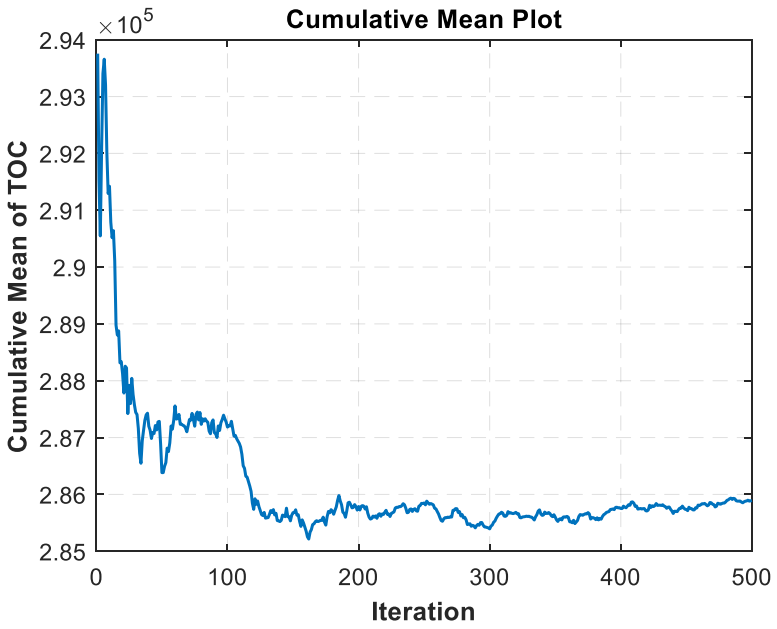

Figure 5.12 The cumulative convergence plot of MCS for TOC

In the MCS procedure, the probabilistic variables include power from solar and wind, as well as electricity and heat load. All probabilistic variables simultaneously

influence the results, making *TOC*, P_E, P_{NG}, P_{FC}, and P_{EL} probabilistic as well. The histogram plot and PDF fitting of TOC are illustrated in Fig. 5.13, with two fitted distributions: normal and Weibull. In this study, the normal distribution is found to be more optimal than the Weibull distribution, as indicated by the log-likelihood value, which has the smallest negative value—determining the best-fitting PDF for this data. The log-likelihood values of both distributions are presented in Table 5.2. Furthermore, the stochastic nature of the analysis introduces additional variability in TOC compared to the deterministic case. Due to the inherent uncertainties in renewable energy generation and demand variations, the probabilistic approach results in a higher TOC than a deterministic model, where all parameters are assumed to be known and fixed. This increase in TOC reflects the cost of accounting for uncertainties and ensuring system reliability under variable operating conditions.

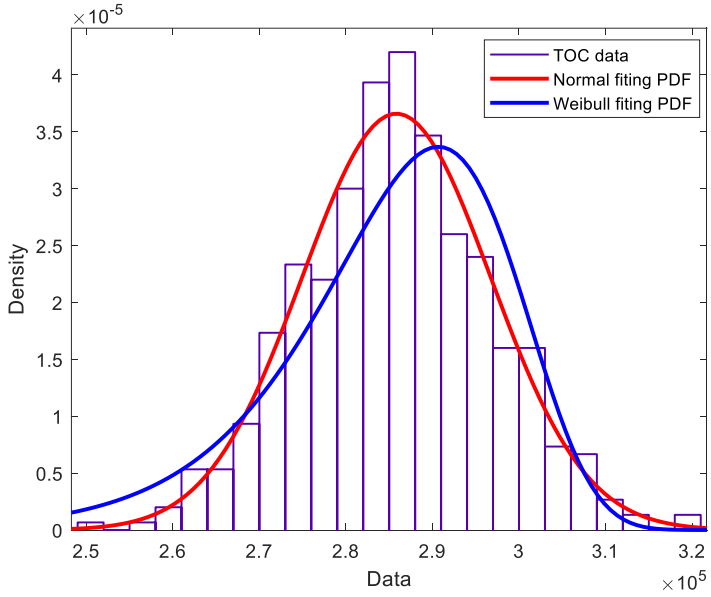

Figure 5.13 The PDF of TOC data

Table 5.2 The TOC log-likelihood of both distribution

Distribution	Normal	Weibull
Log-likelihood	-5,357.38	-5,392.97

The power scheduling results, including power from the grid and NG, are illustrated in Figs. 5.14 and 5.15. Since the data incorporates hourly uncertainties, a box plot should be used for visualization to effectively represent the range of data for each hour. Figures 5.16 and 5.17 illustrate the scheduling of HS under uncertainty conditions. The results highlight variations in power dispatch from EL and FC across different simulation iterations and hours. Additionally, the details of all discussed variables such as power scheduling from electricity, NG, and HS are provided in Appendix B.

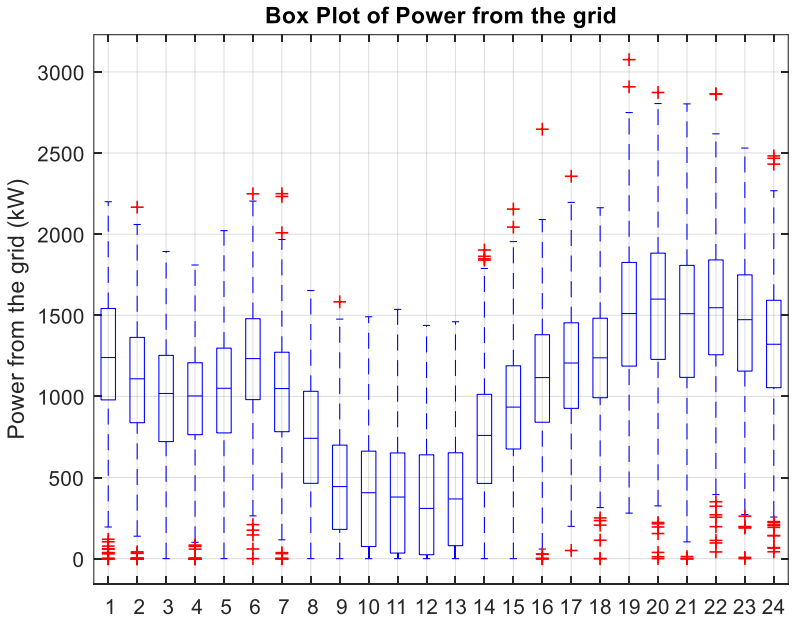

Figure 5.14 The box plot of P_E scheduling solution

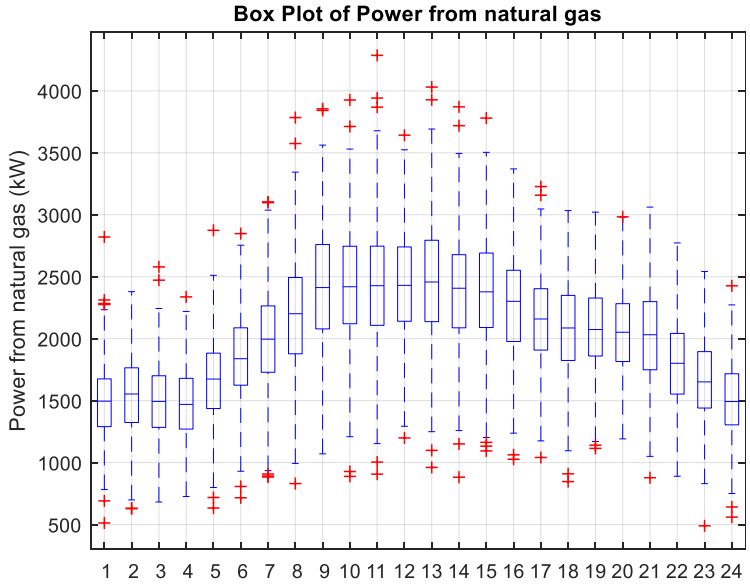

Figure 5.15 The box plot of P_{NG} scheduling solution

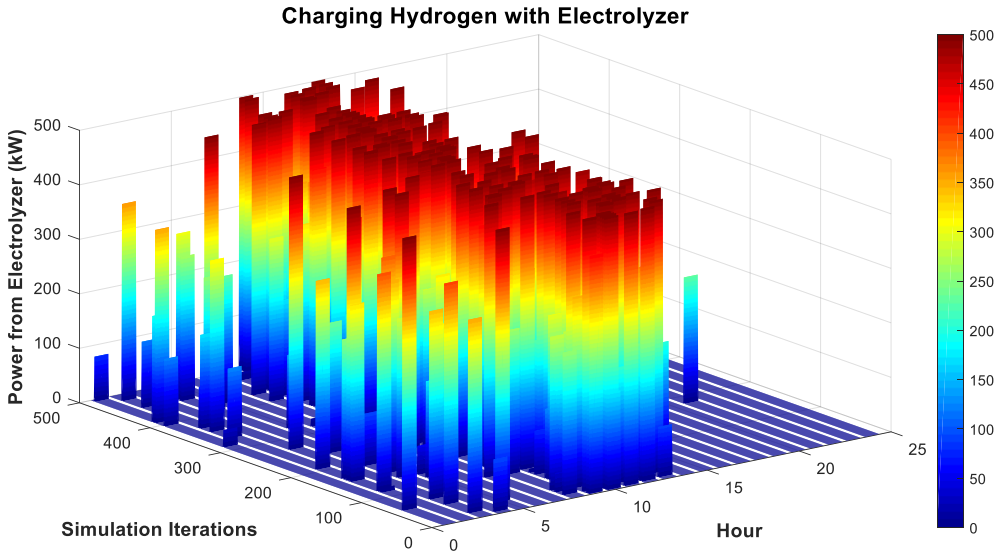

Figure 5.16 The 3D plot of P_{EL} scheduling solution

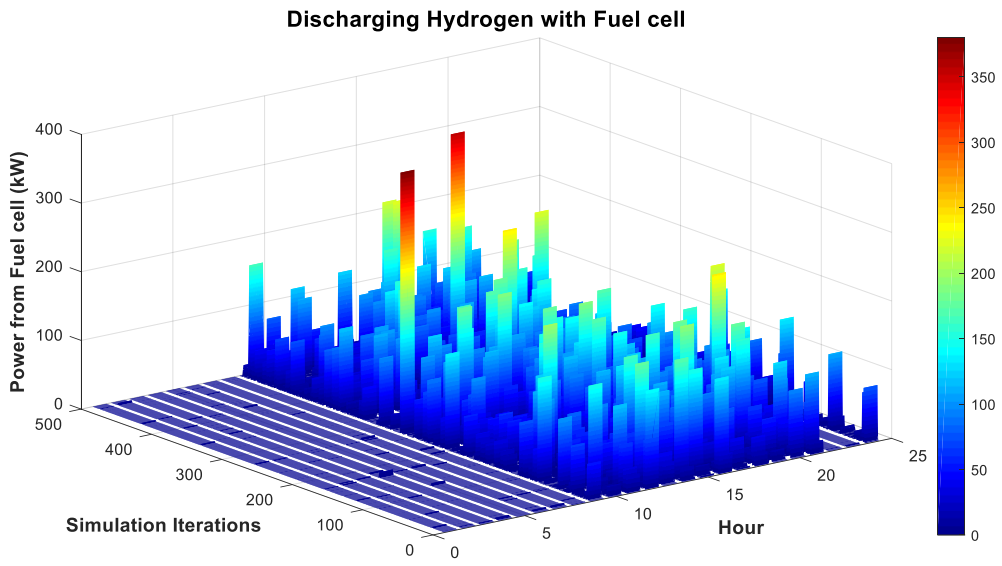

Figure 5.17 The 3D plot of P_{FC} scheduling solution

In Fig. 5.16, the 3D plot of P_{EL} scheduling reveals that the EL operates at higher power levels primarily from the morning to the afternoon. This scheduling pattern is influenced by the availability of surplus RE, particularly wind-solar power, which is more abundant during these hours. EL scheduling tends to reach near-rated power levels, indicating that the system maximizes hydrogen production when excess energy is available. This approach ensures efficient energy utilization and prepares sufficient hydrogen storage for later use. The scheduling also exhibits some variations due to uncertainty, but the general trend remains consistent, favoring high-power operations during periods of high RE generation. On the other hand, Fig. 5.17 illustrates the P_{FC} scheduling, which exhibits a different pattern compared to EL. The FC operates more frequently in the afternoon and night, aligning with periods when electricity demand is higher, and EL does not generate power. Unlike EL, FC does not operate at high power levels but instead follows a strategy of frequent scheduling with relatively low power output. This scheduling behavior ensures a steady supply of electricity from HS while preventing excessive depletion of stored hydrogen. The contrast between P_{EL} and P_{FC} scheduling highlights the coordinated operation of HS, where hydrogen is

efficiently produced and stored during high renewable generation hours and subsequently utilized in a controlled manner to balance the power demand in later hours.

5.5 Chapter Summary

The chapter presents an optimization framework that minimizes TOC and ensures system stability under uncertainty. The integration of WSPHS improves MES performance by efficiently using wind-solar energy and optimizing HS scheduling. The convergence analysis using MCS confirms the approach's robustness, with the final cumulative mean error falling below the 1% threshold. The study emphasizes the importance of stochastic modeling in RE generation and multi-energy demand. This result demonstrates an increase of TOC from the deterministic case, which indicates that the uncertainty influences the objective function. However, the most suitable PDF fitting for TOC in this work is normal distribution due to a lower log-likelihood.